**Andrzej KORDECKI, Henryk PALUS**

Silesian University of Technology, Institute of Automatic Control

# Automatic detection of colour charts in images

***Abstract.*** *This paper presents an algorithm of automatic colour chart detection and colour patch value extraction.The algorithm can detect different types of colour charts in various images. The efficiency of algorithm is measured by successful detection of the X-Rite ColorChecker and compared with the performance of the X-Rite ColorChecker Camera Calibration software. The experimental study shows that proposed algorithm successfully found the colour chart in 77.3% of tested images while the X-Rite software in 53.8% of tested images. The experiments specify optimal image acquisition conditions for successful colour chart detection.*

***Streszczenie****. W artykule przedstawiono algorytm automatycznej detekcji wzornika barw i ekstrakcji wartości barw jego pól. Algorytm umożliwia wykrycie różnych typów wzorników barw w różnych obrazach. Efektywność poprawnej detekcji badano wykorzystując wzornik ColorChecker firmy X-Rite i porównywano z efektywnością detekcji programu X-Rite ColorChecker Camera Calibration. Badania doświadczalne wykazały, że zaproponowany algorytm poprawnie wykrywał wzornik barw w 77,3% badanych przypadków, podczas gdy oprogramowanie firmy X-Rite w 53,8% badanych obrazów. Eksperymenty pozwoliły określić optymalne warunki akwizycji obrazu dla pomyślnej detekcji wzornika barw.****(Automatyczna detekcja wzornika barw w obrazach)***

**Keywords:** automatic detection, colour chart detection, ColorChecker, device characterization.
**Słowa kluczowe**: automatyczna detekcja, detekcja wzornika barw, ColorChecker, charakteryzacja urządzenia.

doi:10.12915/pe.2014.09.49

## Introduction

Many image processing operations require faithful colour information. The areas in which we use information about real colours are: colorimetric calibration, colour constancy, device characterization, white balance and more [1-4]. We can get information about real colours by capturing an image of scene with colour chart (CC). The CC is a card which consists of a number of different colour patches. Reading colour values of CC contained in the image is not difficult, but when we have to repeat this process frequently it becomes a hurdle. It is usually not possible to place the CC in convenient position near colour object of interest in image to make this process easier. Hence, the idea of creating an automatic CC detection and colour patch value extraction algorithm with easy possibility of adding new types of CCs.

The research was focused on detection of X-Rite's ColorChecker Classic (CCC). This chart contains 24 patches, which represent colour samples important in photographic practice. The CCC is a standard colour target. The second tested CC was X-Rite ColorChecker SG (CCSG) that contains 140 colour patches (Fig. 1). The exact description of these CCs can be found on X-Rite's website [5].

Detection of CC is associated with different areas of colour science, but there are not many articles describing methods of CC detection. Colour values of chart patches are usually manually or semi-automatically extracted from the image. The CC detection methods described in the literature often have some restrictions. There are restrictions on light conditions and location of chart in image [6,7]. The CC can be detected, sometimes, with the use of additional supporting elements in scene [8]. Detection methods can be based on searching of white patch and analysis of colour patches saturation for X-Rite ColorChecker Mini [9] or searching based on Canny filter and Hough transform for custom CC [10].

One of the few publications directly on the CC detection is the work [11]. The semi-automatic CC detection presented in this article requires an operator to select the four corners of the chart. On this basis, the methods of projective geometry estimate the coordinates of colour patches. The essence of this method is a multi-stage colour patch detection. In the first step, the colour image is converted to the gray scale image with an additional contrast enhancement by gamma correction and histogram stretching. Next steps are edge detection with Sobel filter, image correction by morphological erosion and thresholding with Otsu's method. Chart patches are localized in the image with the use of information about their dimension ratios. The important step in finding missing patches is a projection of the CC grid on the image. The last step is the calculation of colour patch values by averaging the colour values of pixels belonging to them. Another publication directly about CC detection is the work [12]. The automatic CC detection procedure in this article uses a cost function to find chart in image. Cost function compares colours of chart patches with reference colours and value of standard deviations of the colours within the patch regions. The colour chart model is described by coordinates and colour values of chart patches. In order to find the chart coordinates in image, four corners of chart model are projected on image with the use of Direct Linear Transformation. Coordinates of colour chart are found by minimizing cost function with the use Levenberg-Marquardt algorithm. Procedure can detect colour chart if it is in front of the camera within an allowed operating range. Simpler than the detection task is a problem of CC location in the image. The goal of locating CC is to find the CC coordinates on the basis of local colour descriptors (e.g. colour SIFT) and validation of relevant hypotheses [13].

In the work presented here, an experimental study uses images from two databases: Gehler's database [14] and Silesian University of Technology (SUT) database. There are images taken in different environments: streets, bazaars, exhibitions, shops, forests etc. The images are characterized by various light conditions and different locations of CC. SUT image database have images that may contain different types of CCs in single image, while Gehler's image database contains images with CCC only.

Algorithm of automatic CC detection and colour patch values extraction presented in this paper is universal. It allows to find different types of CCs in single image in various scene conditions. Detection of CC requires the fulfilment of following conditions: each colour patch should have uniform colour and the shape of CC in the image should be a parallelogram.

## Detection algorithm

The proposed here detection algorithm determines the type of CC and locations of colour patches (Fig. 2). Most of the figures presented in this paper depict partial results of

the algorithm performed on the same image. The main steps of the algorithm are described below.

(a) (b)

Fig. 1 X-Rite colour charts: (a) ColorChecker Classic, (b) Digital ColorChecker SG

**Colour quantization and binarization**

The goal of the binarization process is to separate patches from background (Fig. 3). We can easily separate patches, if we process image by colour quantization. Colour quantization eliminates small differences in colour values between image regions with similar colours. Therefore, each patch of chart has a chance to be one region in quantized image. Colour quantization reduces the number of colours in image. It can be performed with the k-means method [16] in following steps:

a) select 25 colours as initial cluster centres,
b) calculate distances between colour pixel values and selected colours,
c) assign colour pixel value to the nearest cluster centre,
d) calculate new cluster centres as arithmetic mean values of colours assigned to colour clusters,
e) if the difference between new and old values of cluster centres is not small - go to point b).

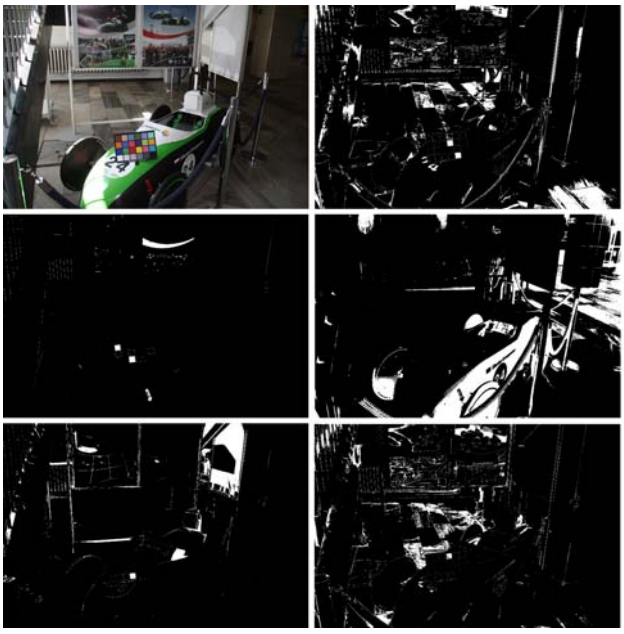

Fig. 3 An example of colour quantization and binarization stage. Original image and 5 selected binary images from 25 resulted images

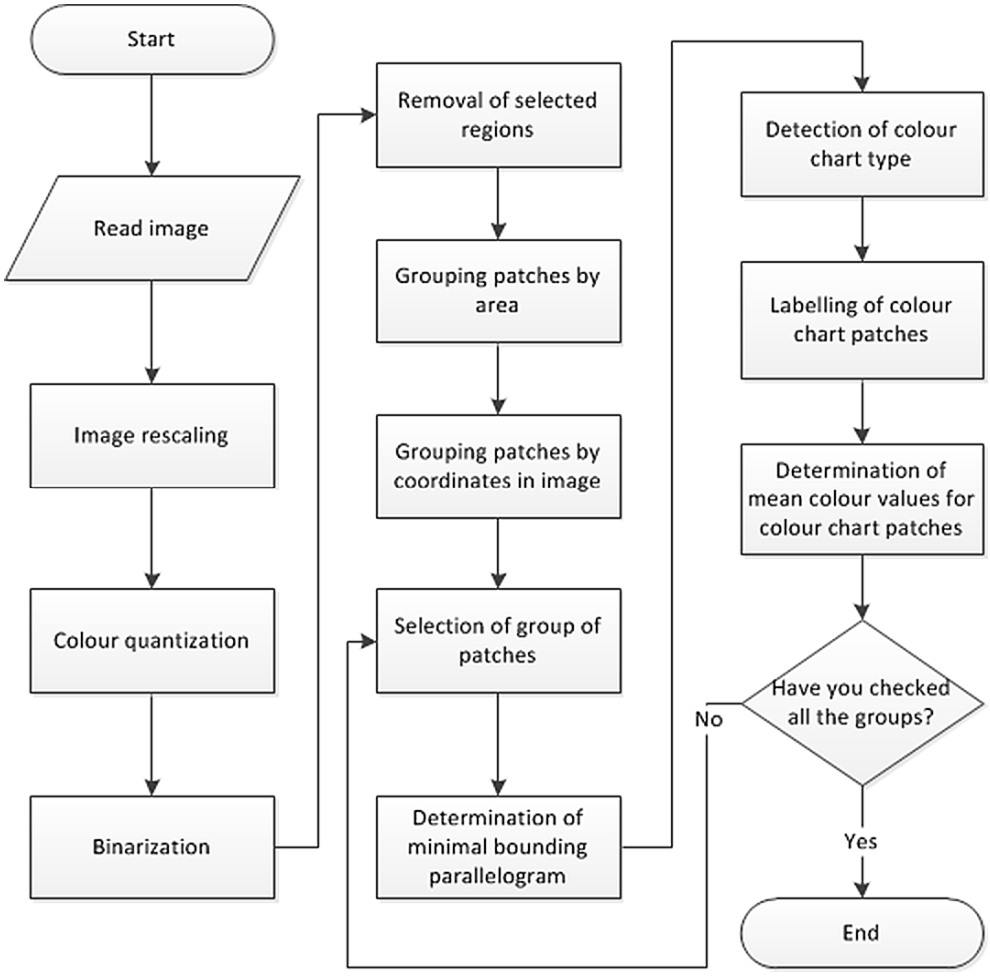


Fig. 2 Flow chart of proposed colour chart detection algorithm [15]

The number and values of initial cluster centres should ensure that even small number of pixels of chart patches will be not included to the cluster containing the pixels in colour of the chart's frame. Therefore, the number and values of initial cluster centres do not have to match the number of patches of specific CC. The initial cluster centres are represented by 24 colour values of CCC patches and an additional black colour. All 25 colours are rescaled to correspond to the maximal colour values of image. The same initial cluster centres were used for detection both CCC and CCSG. The number of colours and values of cluster centres have been established in experiments on SUT image database. It should be noted that in colour quantization process a few clusters may be empty, but this have no significant impact on the whole detection process.

Binarization process assigns each colour a separate binary image. New binary images are formed by checking colour of each pixel in quantized image:

$$I_k = \begin{cases} 1 & I(x,y) = [R_k G_K B_K] \\ 0 & I(x,y) \neq [R_k G_K B_K] \end{cases} \quad (1)$$

where: $I_k(x,y)$ is binary image for $k$-th cluster centre, $I(x,y)$ is colour value of pixel of quantized image in coordinates (x;y), $[R_k G_k B_k]$ is final colour value of $k$-th cluster centre.

In this way each binary image contains the potential colour patches. Because, borders of the CC have a colour different from colour patches, after binarization process we get the patches separated from the frame of CC.

**Removal of selected regions**

Binary images obtained in previous stage have large number of regions. We can improve received binary images by two operations [17]. In the first operation we remove small regions by median filtering with 5x5 pixels window size. Then we perform a morphological closing operation with the same window size to fill small holes in regions. Next we check if the shape of the region is similar to the shape of colour patch. Square shape of chart patches is distorted due to acquisition process and image processing in previous step of algorithm (Fig. 4). In many cases, patches have square shapes with rounded corners.

The regions are examined by the use of the Euler number [18], which must be equal to one (region without "holes"). The second condition for region checking is proper value of circularity factor [19]:

$$0.65 < \frac{4\pi A}{P^2} < 0.95 \quad (2)$$

where: $A$ is region's area, $P$ is region's perimeter.
Regions that do not meet above conditions are removed (Fig. 5).

**Patch grouping**

Previous stage, however, did not remove all the regions that are not potential patches. In order to detect a colour chart, geometrical properties of colour patches can be used (size and location). We used for that purpose a hierarchical clustering algorithm [20]. The grouping is based on differences in areas between potential patches:

$$\Delta A_{ij} = \left| A_i - A_j \right| \quad (3)$$

where: $\Delta A_{ij}$ is the absolute difference between $i$-th and $j$-th areas, $A_i$ and $A_j$ are the areas of $i$-th and $j$-th potential patches.

Fig. 4 Examples of chart patches after binarization process

(a)

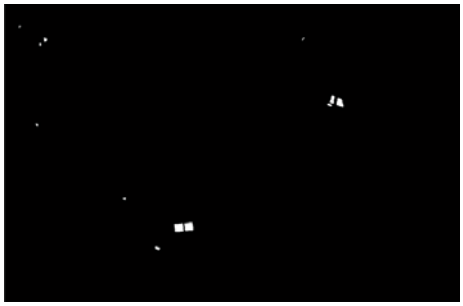

(b)

Fig. 5 Example of image after binarization process (a) and after removal of selected regions (b)

First, we join the patches with the smallest absolute difference between areas. Patches are joined to groups as long as the relative differences between the mean areas of both groups are less than 30%:

$$\left| \frac{\overline{A_n} - \overline{A_m}}{\overline{A_n}} \right| < 0.3 \qquad \left| \frac{\overline{A_n} - \overline{A_m}}{\overline{A_m}} \right| < 0.3 \quad (4)$$

where Am and An are the mean areas of $m$-th and $n$-th groups.

If the threshold would be bigger, the groups will include objects which are not patches. If the threshold would be smaller, the groups will be too small and will be harder to detect the colour chart in the next steps of algorithm. The patch grouping process ends, when it no longer can create a new group (Fig. 6).

Colour patches belonging to the same CC are near each other. The obtained groups of patches with similar area are then grouped based on the coordinates in the image (Fig. 6). The goal of this step is to remove the elements of group which do not belong to chart patches. This grouping is done with hierarchical clustering using the Euclidean distance between coordinates of centroids of two groups. Similarly to the previous clustering method, we first join groups with the smallest distance between their centroids. But, the stop criterion is now a number of formed groups: 1, 2, ..., 8. We assumed the final number of groups as eight. These both clustering methods define the groups of potential patches for further processing.

**Detection of colour chart type**

The rectangular shape of CC can be distorted by various image acquisition conditions. Therefore we assume that the shape of parallelogram is the best simplification of

shape of distorted CC. The parallelogram without distortions is a rectangle. We can determine the type of colour chart by checking the following properties:

- the number of colour patches,
- the ratio between the length of the shorter and the longer sides of minimal bounding parallelogram,
- the ratio between the mean square root of patch area and the length of the longer side of minimal bounding parallelogram,
- the ratio between the mean square root of patch area and the length of the shorter side of minimal bounding parallelogram.

If the tested group meets all the above requirements we will find a specific type of colour chart. We determine minimal bounding parallelogram (Fig. 7) with the use of algorithm described in [21] on convex hull [22] of patch groups. Based on coordinates of parallelogram are determine information about the length of shorter and longer sides of parallelogram.

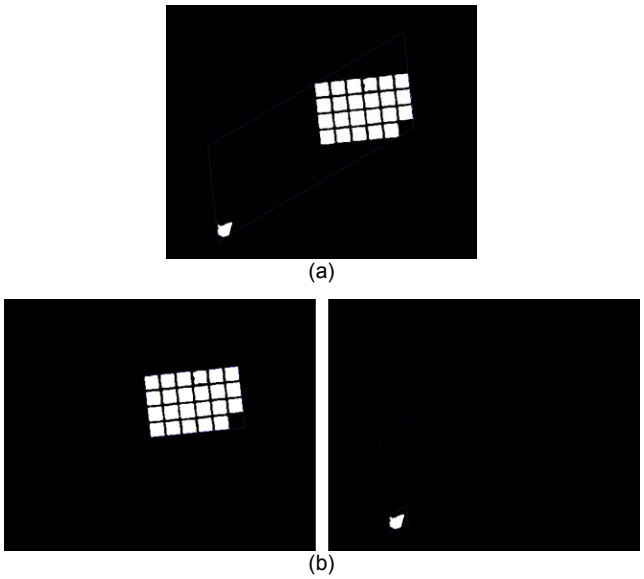

(a)

(b)

Fig. 6 Grouping of potential patches by area (a) and by coordinates (b).

**Labelling of colour patches**

The first step in determining a location of each colour patch is initial labelling. We can see an example of initial labelling on image containing CC with shape distortion (Fig. 7). This stage of algorithm uses data about location and proportions of CC patches in form of CC grid. Therefore, the algorithm to detect a new type of CC needs only information about CC grid. The initial labelling (Fig. 8) is performed by projecting points representing the corners of CC grid on the corners of a bounding parallelogram known from the previous stage. The Direct Linear Transformation that allows transforming any coordinates to coordinates of image is based on principles of affine geometry. Each point in the affine geometry is represented by three spatial coordinates (*x,y,1*) and the same point in Euclidean geometry is represented by two coordinates (*x,y*). The point (*kx,ky,k*) describes the same point for each non-zero value of *k*. We perform the Direct Linear Transformation in the following steps [23]:

a) determine at least four points with coordinates (*x,y,z*) in projected image and the same number of matching points on desired position with coordinates (*x',y',z'*) in detected image. Assume following pairs of points in labelling process:
   - initial labelling: (*x,y,z*) represents corners of CC grid and (*x',y',z'*) represents corners of minimal bounding parallelogram found in detected image,
   - final labelling: (*x,y,z*) represents centres of CC grid patches and (*x',y',z'*) represents centres of actual CC patches found in detected image.

   In case of two-dimensional images the coordinates *z* and *z'* should be equal 1. Assume the following transformation matrix *H*:

$$\begin{bmatrix} x' \\ y' \\ z' \end{bmatrix} = \begin{bmatrix} h_{11} & h_{12} & h_{13} \\ h_{21} & h_{22} & h_{23} \\ h_{31} & h_{32} & h_{33} \end{bmatrix} \begin{bmatrix} x \\ y \\ z \end{bmatrix} \tag{5}$$

   where: $h_{11};h_{12};\ldots,h_{33}$ are elements of *H*.

b) for z = z' = 1 we transform the previous equations:

$$\begin{cases} x' = \dfrac{h_{11}x + h_{12}y + h_{13}}{h_{31}x + h_{32}y + h_{33}} \\ y' = \dfrac{h_{21}x + h_{22}y + h_{23}}{h_{31}x + h_{32}y + h_{33}} \end{cases} \tag{6}$$

   After small modifications of equations (6) we obtain:

$$\begin{aligned} h_{11}x - h_{31}xx' + h_{12}y - h_{32}yx' + h_{13} - h_{33}x' = 0 \\ h_{21}x - h_{31}xy' + h_{22}y - h_{32}yy' + h_{23} - h_{33} = 0 \end{aligned} \tag{7}$$

   We can write elements of equations (7) in matrix form:

$$\Theta_i = \begin{bmatrix} x_i & 0 & -x_i x_i' & y_i & 0 & -y_i x_i' & 1 & 0 & -x_i' \\ 0 & x_i & -x_i y_i' & 0 & y_i & -y_i y_i' & 0 & 1 & -y_i' \end{bmatrix} \tag{8}$$

$$h = \begin{bmatrix} h_{11} & h_{21} & h_{31} & h_{12} & h_{22} & h_{32} & h_{13} & h_{23} & h_{33} \end{bmatrix}^T$$

   where: $(x_i,y_i)$ is *i*-th point in projected image, $(x_i',y_i')$ is *i*-th point in detected image.

   Matrix for pairs of points is as follows:

$$\Theta = \begin{bmatrix} \Theta_1 & \Theta_2 & \ldots & \Theta_i & \ldots & \Theta_n \end{bmatrix}^T \tag{9}$$

   where: *n* is a number of pairs of points, e.g. 4 pairs of points in initial labelling.

c) we can calculate nine unknown elements of matrix h:

$$\begin{cases} \min_h \|\Theta h\|^2 \\ \|h\| = 1 \end{cases} \tag{10}$$

   The solution of above task is a matrix D coming from Singular Value Decomposition method [24]:

$$\Theta = SVD^T \tag{11}$$

   where: Q is an n×9 matrix, S is an n×n unitary matrix, V is an n×9 diagonal matrix with nonnegative real numbers on the diagonal and DT is a 9×9 unitary matrix that contains the elements of matrix h.

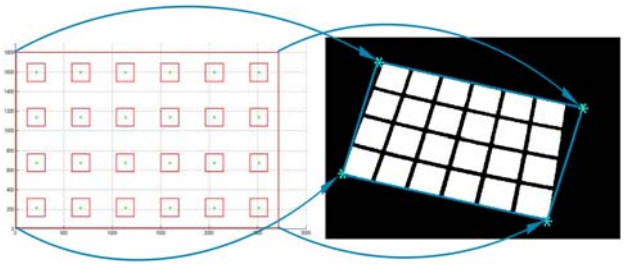

(a) (b)

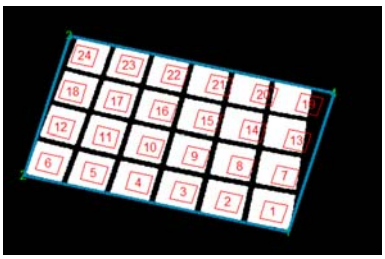

(c)

Fig. 7 Example of initial labelling: (a) the colour chart grid, (b) minimal bounding parallelogram with marked corners, (c) results of initial labelling

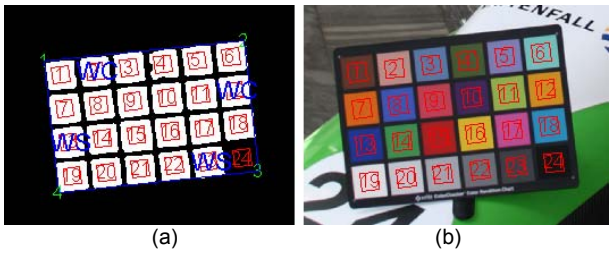

(a) (b)

Fig. 8 Result of: (a) initial labelling, (b) colour chart detection

In initial labelling we also transform coordinates of centres of CC grid patches onto corresponding coordinates in the image. Then we calculate the distances between all patch centres in the image and transformed centres of CC grid patches. The shortest distances between centres determine the ordinal numbers of colour patches. Because initial coordinates of colour patches could be inaccurate, we repeat once again the calculation of transformation matrix based on new precise coordinates of centres of patches (Fig. 8).

The colour values of chart patches are compared in order to determine which patch on corners of parallelogram has the first ordinal number. Now we have all geometric data to determine the mean colour values for all colour patches.

**Experiments and results**

The effectiveness of the proposed colour chart detection algorithm was compared with the detection results of X-Rite's ColorChecker Camera Calibration software [5]. Detection of CCs was rated according to the following rank scale (1): 0 - no detection, 1 - incorrect detection, 2 - correct detection of colour chart. The incorrect detection of colour chart occurs when the algorithm correctly detects the type of colour chart, but its coordinates with some defects, e.g. at least one patch contains chart frame pixels. If the image contains more than one CC we recognize each colour chart separately. The X-Rite software was not able to detect more than one colour chart in the same image and allows to detect few types of CCs only (Fig. 9). Therefore, we have not compared the performance of detection algorithm for SUT image database that contains images with more than one colour chart in single image.

Fig. 9 Detection of two types of colour charts in single image

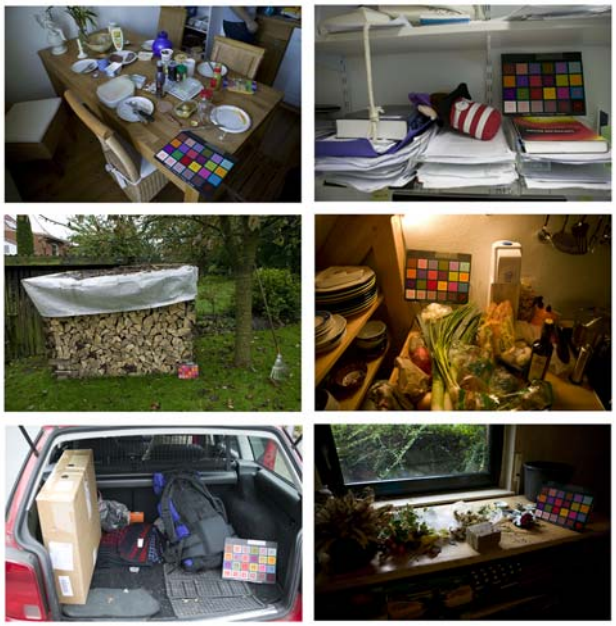

Fig. 10 Examples of images with successful colour chart detection

Table 1. Comparison of colour chart detection results

| Image database | Colour Chart | Rank scale | | | Detection Rate |
|---|---|---|---|---|---|
| | | 0 | 1 | 2 | |
| Proposed algorithm | | | | | |
| Gehler's[13] | CCC | 110 | 19 | 440 | 77.3% |
| SUT | CCC | 15 | 3 | 55 | 75.3% |
| | CCSG | 14 | 4 | 20 | 52.6% |
| X-Rite software | | | | | |
| Gehler's[13] | CCC | 241 | 22 | 306 | 53.8% |
| SUT | CCC | 30 | 4 | 39 | 53.4% |

Chart detection results show an advantage of proposed detection algorithm over X-Rite's algorithm. The difference was quite significant and proposed detection algorithm had about 23% more correct detections. Our algorithm was more robust to various scene conditions (Fig. 10).

Presented detection algorithm can detect CCs even if few patches are concealed (Fig. 11). The differences between proposed algorithm and X-Rite's algorithm are forming probably in early stages of CC detection. In Fig. 12a-b we can see the CC without deformations, but one of the compared algorithms did not find the chart. In proposed algorithm the reason of bad detection is the small number of detected patches. Unsuccessful detection of colour chart by X-Rite's algorithm is probably caused by lower tolerance in deviation of size and shape of CC.

The reasons of main difficulties in CC detection are a deformation of shape of CC and a small size of chart in the image. The deformation of shape of CC is connected with orientation and location of chart in the image. It can change the actual rectangular shape into the nonlinear shape (Fig.12a). Distortions are made by: location of colour chart, not rigid material of colour chart and camera optics. Due to the small number of pixels representing the chart patches

the algorithm has the small influence on quantization process and has deformed shapes of colour patches (Fig. 12b). Therefore, CCs should be clearly visible in image. Influence on the proper detection have also the light conditions. The ambient light causes changes in the colour values and high colour variations due to nonuniformity. The lower detection rate of CCSG was caused by the smaller size of chart patches in the image in comparison to CCC. If the size of CCSG patches in the tested images would be similar to size of CCC patches, probably the rate of detection of these two charts would be comparable.

Fig. 11 Examples of images with successful colour chart despite the masking of few patches

(a)

(b)

Fig. 12 Examples of images with: (a) successful detection by proposed algorithm only, (b) successful detection by X-Rite algorithm only

## Conclusion

The proposed detection algorithm allows to work faster and more stable in comparison to manual reading of colour information from the image containing the CC. Proposed algorithm can detect more than one colour chart on the same image in different scene conditions. Detection rate of proposed algorithm was higher than in case of X-Rite software and was respectively 77.3% to 53.8% of tested images. The research allowed to identify scene conditions for successful CC detection. The algorithm can correctly detect the CC when it occupies at least 10% of the image area for CCC and 20% for CCSG, and the colour chart is perpendicular to the optical axis of the camera.


### *Acknowledgments*

*This work was supported by Polish Ministry for Science and Higher Education under internal grant BK/Rau1/2013 for Institute of Automatic Control, Silesian University of Technology, Gliwice, Poland.*


## REFERENCES


[1] H. R. Kang, Color Technology for Electronic Imaging Devices, SPIE Optical Engineering Press (1997)

[2] G. Sharma, Digital Color Imaging Handbook, CRC Press (2003).

[3] H.-C. Lee, Introduction to Color Imaging Science, Cambridge University Press (2005)

[4] A. Kordecki, H. Palus and A. Bal, Colorimetric calibration in the image acquisition process, Przegląd Elektrotechniczny, nr 4, 80-83, 2013 (in Polish)

[5] X-Rite, X-Rite ColorChecker Camera Calibration (2012)

[6] N. K. Vuong, S. Chan, and C. T. Lau, Classification of pH levels using a mobile phone, in Proceedings of the 13th IEEE Intern.l Symposium on Consumer Electronics, 823–827, (2009)

[7] M. Liu, I. Konya, J. Nandzik, S. Eickeler, N. Flores-Herr, and P. Ndjiki-Nya, A new quality assessment and improvement system for print media, EURASIP Journal on Advances in Signal Processing 109, 1–17, (2012)

[8] N. Joshi, Color calibration for arrays of inexpensive image sensors, Tech. Rep. CSTR 2004-02 3/31/04 4/4/04, Stanford University, Department of Computer Science (2004)

[9] S. Van Poucke, Y. Haeghen, K. Vissers, T. Meert, and P. Jorens, Automatic colorimetric calibration of human wounds, BMC Medical Imaging 10(1), 1–11, (2010)

[10] B. Streckel, Colorimetric calibration of CCD - video camera under real conditions with the methods of color management, Master's Thesis, University of Kiel, Germany (1999)

[11] T. Tajbakhsh, R.-R. Grigat, Semiautomatic color checker detection in distorted images, in Proceedings of the 5th IASTED International Conference on Signal Processing, Pattern Recognition and Applications, 347–352, (2008)

[12] A. Ernst, A. Papst, T. Ruf, and J.-U. Garbas, Check my chart: A robust color chart tracker for colorimetric camera calibration, in Proceedings of the 6th International Conference on Computer Vision / Computer Graphics Collaboration Techniques and Applications, MIRAGE, 5:1–5:8, (2013)

[13] S. Bianco, C. Cusano, Color target localization under varying illumination conditions, Lecture Notes in Computer Science 6626, 245–255, (2011)

[14] P. Gehler, C. Rother, A. Blake, T. Minka, and T. Sharp, Bayesian color constancy revisited, in Proceedings of the IEEE Conf. on Computer Vision and Pattern Recognition, 1–8, (2008)

[15] A. Kordecki, Colorimetric calibration procedures for image acquisition devices, Ph.D. Thesis, Silesian University of Technology, Gliwice, 2013 (in Polish)

[16] J. MacQueen, Some methods for classification and analysis of multivariate observations, in Proceedings of 5th Berkeley Symposium on Mathematical Statistics and Probability, University of California Press, 281–297, (1967)

[17] R. C. Gonzalez, R. E. Woods, Digital Image Processing, Prentice Hall (2002)

[18] W. K. Pratt, Digital Image Processing: PIKS Inside, John Wiley & Sons (2007)

[19] W. Burger and M. J. Burge, Principles of Digital Image Processing, Springer (2009)

[20] J. Han, M. Kamber, and J. Pei, Data Mining: Concepts and Techniques, Morgan Kaufmann (2006)

[21] C. Schwarz, J. Teich, A. Vainshtein, E. Welzl, and B. L. Evans, Minimal enclosing parallelogram with application, in Proceedings of 11th Annual Symposium on Computational Geometry, 434–435, (1995)

[22] R. L. Graham, An efficient algorithm for determining the convex hull of a finite planar set, Information Processing Letters 1, 132–133, (1972)

[23] R. Hartley, A. Zisserman, Multiple View Geometry in Computer Vision, Cambridge University Press (2004).

[24] W. H. Press, S. A. Teukolsky, W. T. Vetterling, and B. P. Flannery, Numerical Recipes: The Art of Scientific Computing, Cambridge University Press (2007)



*Authors: dr inż. Andrzej Kordecki, dr hab. inż. Henryk Palus, Prof. Pol. Śl., Institute of Automatic Control, Silesian University of Technology, Akademicka 16, 44-100 Gliwice, Poland, email: andrzej.kordecki@polsl.pl, henryk.palus@polsl.pl.*